



Cite this: DOI: 10.1039/d5sc05141j

All publication charges for this article have been paid for by the Royal Society of Chemistry

Light responsive hydrogen selenide (H₂Se)/hydrogen diselenide (H₂Se₂) donors: applied for protein S-selenylation on PRDX6

Biswajit Roy,^{†a} Eshani Das,^{†a} Meg Shieh,^a Seiryu Ogata,^b Minkyung Jung,^b Hiroaki Fujita,^c Sen Zhang,^a Jerome R. Robinson,^a Takaaki Akaike^b and Ming Xian^{*,a}

Hydrogen selenide (H₂Se) is an important metabolite in selenium biochemistry and plays a crucial role in redox biology. While its significance has become increasingly recognized, research on H₂Se is challenging due to its instability and high reactivity. Suitable compounds (aka donors) that can selectively produce H₂Se in biological systems would facilitate this research field. In this work, we explored photo-triggered H₂Se donors by utilizing two structural templates: 2-nitrobenzyl selenides and 2-methoxy-6-naphthacyl selenides. The photoreactions of these compounds under light were studied. 2-Nitrobenzyl selenides were found to release H₂Se (and its oxidized form H₂Se₂) slowly under UV light, but the released H₂Se/H₂Se₂ could further react with the photoproduct and be consumed. On the other hand, naphthacyl selenides could undergo clean and fast reactions to produce H₂Se/H₂Se₂, as well as a stable and fluorescent photoproduct. This self-monitoring and quick releasing ability make naphthacyl selenides 'smart donors' for biological applications. Importantly, this donor was found to induce protein S-selenylation (CysS-SeH) on Cys47 and Cys91 in both recombinant peroxiredoxin-6 (PRDX6) and PRDX6-overexpressing HEK293T cells. This photo-triggered donor system may serve as a new strategy to control selenium-based protein post-translational modifications for mechanistic studies into selenium metabolic pathways and ferroptosis.

Received 10th July 2025
Accepted 12th September 2025

DOI: 10.1039/d5sc05141j

rsc.li/chemical-science

Introduction

Selenium is an essential trace element.¹ While selenium deficiency has been linked to diseases including Keshan disease and Kashin-Beck disease,² an overdose of selenium (more than 400 µg per day) can lead to acute selenosis that causes nausea, hair and nail loss, disorders of the nervous system and skin, poor dental health, *etc.*³ Thus, both selenium's health benefits and toxic effects are highly concentration dependent.⁴ In the human body, the physiological function of selenium is served through 25 selenoproteins with selenocysteine at their active sites.⁵ These include redox enzymes like glutathione peroxidase (GPx) and thioredoxin reductases (TrxR). Selenium is accumulated in the body from dietary sources containing selenomethionine (SeMet), selenocysteine (Sec), selenite (SeO₃²⁻), and selenate (SeO₄²⁻), all of which are hypothesized to produce

hydrogen selenide (H₂Se) in their metabolic pathways.^{6–8} H₂Se is also known to be the Se source of selenophosphate synthetase (SPS), which contributes to selenophosphate (SePO₃³⁻) production and the subsequent synthesis of Sec and selenoproteins. Through different enzymatic and/or redox reactions, H₂Se is believed to play important regulatory roles in biological systems.⁸ It should be noted that H₂Se is a highly reactive species and a strong reductant (its reduction potential is comparable to that of H₂).⁹ Although the implications of H₂Se *in vivo* have not yet been clearly demonstrated, the administration of exogenous H₂Se (using sodium hydroselenide (NaHSe) as the equivalent) has shown some interesting activities.¹⁰ For instance, it was found that H₂Se can decrease O₂ consumption in the rat soleus muscle and liver and induce transient inhibition on mitochondrial cytochrome C oxidase. H₂Se also showed cytoprotective effects against H₂O₂-induced toxicity. Furthermore, H₂Se increased the expression of selenoproteins in human hepatocytes while its oxidized form (*e.g.* sodium selenite) exhibited opposite effects.

The studies on H₂Se so far have led some researchers to suggest that H₂Se may be a possible gasotransmitter,¹¹ analogous to hydrogen sulfide (H₂S).¹² H₂S has many physiological functions related to redox homeostasis. One of the important functions of H₂S is to induce protein persulfidation (forming

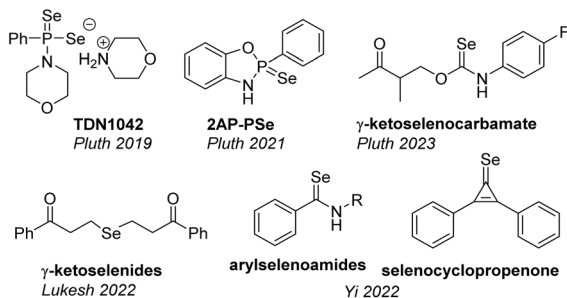
^aDepartment of Chemistry, Brown University, Providence, Rhode Island 02912, USA.
E-mail: ming_xian@brown.edu

^bDepartment of Redox Molecular Medicine, Tohoku University Graduate School of Medicine, 2-1 Seiryomachi, Aobaku, Sendai 980-8575, Japan

^cDepartment of Molecular and Cellular Physiology, Kyoto University School of Medicine, Kyoto, Japan

[†] B. R. and E. D. contributed equally.





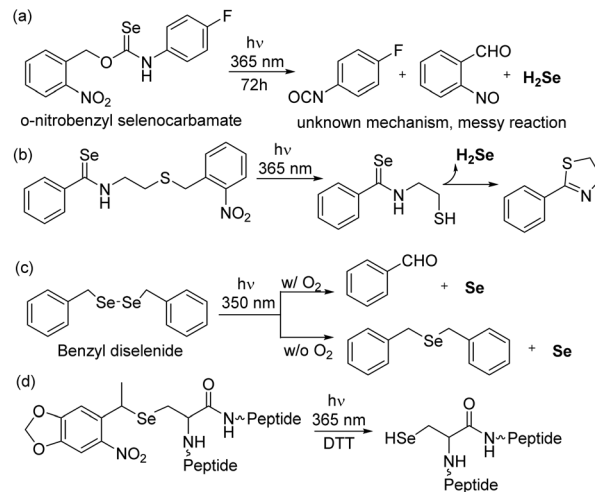
Scheme 1 The structures of reported H_2Se donors.

protein-SSH on protein cysteine residues), an important post-translational modification.¹³ Similarly, H_2Se is likely to induce protein *S*-selenylation (forming protein-SSeH). Recently, studies have reported that *S*-selenylation can be induced on peroxiredoxin 6 (PRDX6), a key regulator of ferroptosis.^{14,15} Significantly, this modification enables PRDX6 to act as a selenium-acceptor protein to facilitate intracellular selenium utilization and thereby guide ferroptosis sensitivity in cells. In H_2S research, synthetic H_2S donors play critical roles, and many such donors have been developed.¹⁶ H_2Se donors are also needed for the exploration of H_2Se , but this is a very underdeveloped field. To date, only a few H_2Se donors (Scheme 1) have been reported, and the design of these compounds is largely based on known H_2S donors. For instance, Pluth *et al.* prepared Se analogs of two popular hydrolysis-based H_2S donors GYY4137 (ref. 17) and FW1256.¹⁸ The resulting H_2Se donors are TDN1042 (ref. 19) and 2AP-PSe,²⁰ respectively. The same group also reported base-mediated donors γ -ketoselenocarbamates.²¹ Lukesh *et al.* reported pH-controlled H_2Se release from bis- γ -keto selenides based on β -elimination.²² Yi *et al.* reported cysteine-mediated H_2Se release from selenocyclopropenones and selenoamides under physiological pH.²³ These compounds have been used to reveal some interesting activities of H_2Se such as anticancer and antioxidant effects. Our laboratory seeks to develop novel H_2Se donors with improved spatiotemporal control in biological settings. To this end, we are particularly interested in light-triggered donors. Herein, we report the discovery of a promising, unique template and its application in inducing protein *S*-selenylation.

Results and discussion

The idea of photo-triggered and C–Se bond cleavage-based donors

To date, reliable photo-triggered and C–Se bond cleavage-based H_2Se donors are still missing. While two photo-triggered H_2Se donors have been reported, they do not involve photo-induced C–Se bond cleavage. In one example, Pluth *et al.* reported a photo reaction of *o*-nitrobenzyl selenocarbamate in which C–O bond cleavage occurred and subsequently produced H_2Se (Scheme 2a).²¹ As the authors noted, there were several limitations: (1) the reaction was not clean and needed a very long light exposure time (72 h) to release H_2Se , and (2) the reaction mechanism was unclear. The release of H_2Se did not appear to



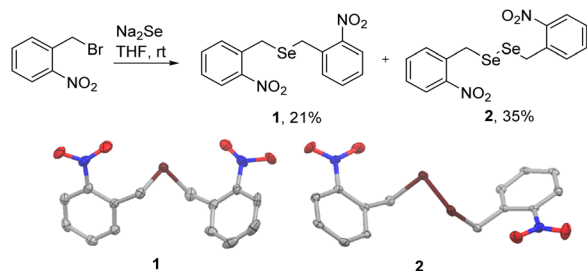
Scheme 2 Reported photo-triggered H_2Se donors (a and b) and photo-triggered C–Se bond cleavage reactions (c and d).

involve the formation of COSe, which was different from the thiocarbamate analogs (generating COS as the key intermediate). In another example, Yi *et al.* employed a photo-triggered thiol formation to promote an intramolecular reaction with arylselenoamide to release H_2Se (Scheme 2b).²⁴ However, the H_2Se -releasing efficiency of this donor was not high, likely due to the consumption of the released H_2Se by the photo-byproduct *o*-nitroso benzaldehyde. In addition, since the arylselenoamide is known to release H_2Se in the presence of cysteine, the specificity of this photo-release process may be compromised. In the search for photo-triggered C–Se bond cleavage reactions, we noticed that both Se–Se and C–Se bonds can break under light irradiation for certain structures. For example, the photo-irradiation of benzyl diselenide at 350 nm (Scheme 2c) led both the Se–Se and C–Se bonds to break, which produced dibenzyl selenide in the absence of oxygen and benzaldehyde in the presence of oxygen, along with the elemental selenium Se^0 .²⁵ Another work by Otting *et al.* showed that 4,5-dimethoxy-2-nitrobenzyl group could promote C–Se bond cleavage under UV light to generate selenocysteine residues in selenoproteins (Scheme 2d).²⁶ These results suggest that photo-triggered C–Se bond cleavage to release H_2Se is possible, but suitable photoremovable protecting groups (PRPGs) need to be identified. As such, we sought to explore direct C–Se bond cleavage-based strategies to release H_2Se .

The study of bis-nitrobenzyl-diselenide and -monoselenide

The *o*-nitrobenzyl group is one of the most widely used PRPGs and has been applied in the release of many bioactive molecules, primarily through C–O bond cleavage.²⁷ We first attempted to prepare bis-2-nitrobenzyl monoselenide **1** under the expectation that it would be able to release H_2Se . However, the preparation (treating 2-nitrobenzyl bromide with sodium selenide, Scheme 3) produced considerable amounts of diselenide **2** along with monoselenide **1**. Their structures were characterized by NMR and X-ray crystallography. In theory,



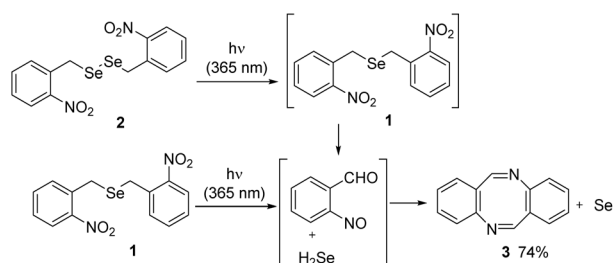


Scheme 3 Preparation of *o*-nitrobenzyl mono- and di-selenides (1 and 2). Thermal ellipsoid plots of 1 and 2 displayed at 50% probability.

compound 1 can be considered a H_2Se donor while compound 2 can be considered a H_2Se_2 donor. However, we realized that H_2Se was highly sensitive to oxygen and would eventually be oxidized to Se^0 , likely *via* H_2Se_2 as the intermediate. On the other hand, if H_2Se_2 was formed, it would disproportionate quickly to H_2Se and Se^0 , as suggested by Lukesh *et al.*²² Thus, both the monoselenide and the diselenide (1 and 2) may lead to similar outcomes under a photo-triggered release; we decided to test both compounds in our studies.

The photoreactions of compounds 1 and 2 were carried out under 365 nm 100 W LED light, and the progress was monitored by ^1H NMR (Fig. S1 and S2). When diselenide 2 was irradiated with light, we initially observed a clean conversion to form monoselenide 1. However, compound 3 (ref. 28) was identified as the final product, along with the formation of red elemental selenium (Scheme 4), which was confirmed by reacting this species with triphenylphosphine (PPh_3) to form triphenylphosphine selenide ($\text{Se}=\text{PPh}_3$). When monoselenide 1 was irradiated under the same conditions, we did not observe the formation of diselenide 2 while compound 3 was again formed along with the elemental selenium Se^0 . Our observation of forming 1 from 2 under light was similar to the reported photoreaction of benzyl diselenide,²⁵ which indicated that a radical pathway was involved in the conversion of diselenide 2 to monoselenide 1 as described in Scheme 5.

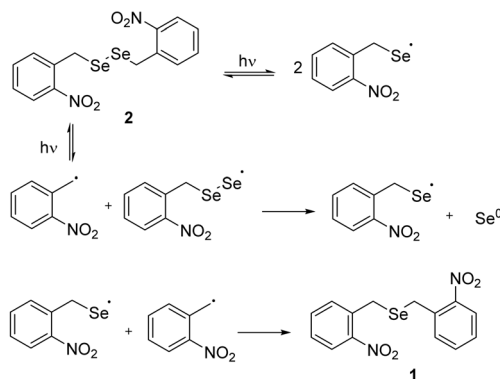
The conversion from 1 to 3 should proceed *via* the classical anionic pathway of the nitrobenzyl-PRPG to form *o*-nitroso benzaldehyde 4 and H_2Se . However, we did not observe 4 in the reaction mixture likely because H_2Se (a strong reducing agent) reduced the nitroso group of 4 to form 2-aminobenzaldehyde, which then self-condensated to form compound 3. To validate the H_2Se release from 1, we carried out a trapping experiment



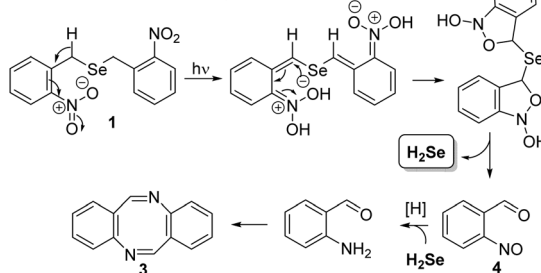
Scheme 4 Photolysis of 1 and 2 under LED light.

Proposed mechanism

First step: Radical pathway



Second Step: Anionic pathway



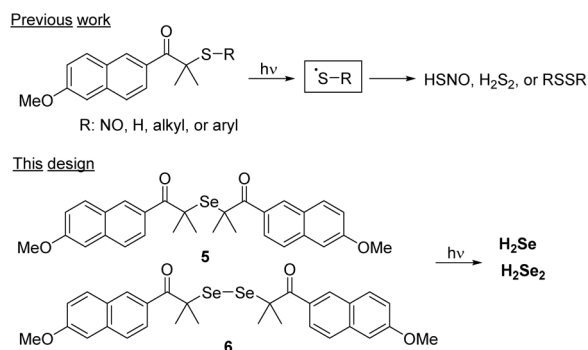
Scheme 5 Proposed mechanisms of the photoreactions of 1 and 2.

with benzyl bromide (BnBr). Interestingly, we only observed a trace amount of formation of Bn_2Se_2 and Bn_2Se . This indicated that the reduction of 4 with H_2Se was much faster than that of the trapping reaction of H_2Se . Therefore, nitrobenzyl was not a suitable PRPG for the design of $\text{H}_2\text{Se}/\text{H}_2\text{Se}_2$ donors.

Design and synthesis of naphthacyl-derived selenides

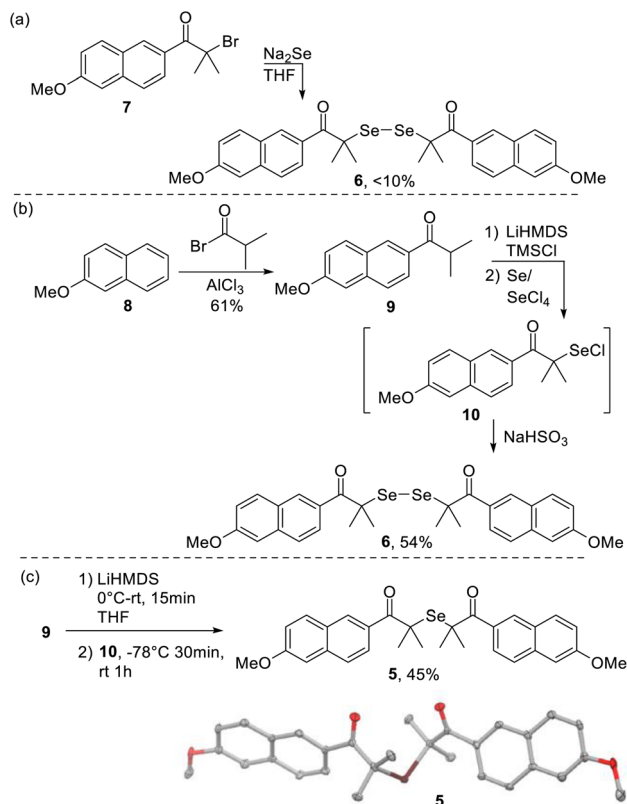
Our recent work revealed that naphthacyl-derived sulfur-containing compounds can undergo clean and fast C–S bond cleavage to release sulfur species under light (Scheme 6).^{29–31} We wondered if this PRPG could also be used to design photo-triggered $\text{H}_2\text{Se}/\text{H}_2\text{Se}_2$ donors (*e.g.* monoselenide 5 and diselenide 6) and prepared these compounds accordingly.

Our first attempt was to directly treat a known naphthacyl bromide 7 with Na_2Se (Scheme 7a). However, this reaction gave



Scheme 6 The design of naphthacyl-derived selenides 5 and 6.



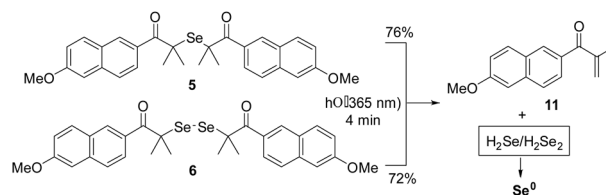


Scheme 7 (A) Reaction of **7** with Na_2Se . (B) Synthesis of naphthacyl-derived diselenide **6**. (C) Synthesis of naphthacyl-derived monoselenide **5** and thermal ellipsoid plot of **5** displayed at 50% probability.

the diselenide **6** in a low yield (10%) and no monoselenide **5** was observed. Next, we tried the installation of selenium on a naphthacyl ketone **9**,³² which was prepared *via* Friedel–Crafts acylation of 2-methoxynaphthalene **8**. The TMS silyl enol ether generated from **9** was treated with Se/SeCl_4 which should provide selenenyl chloride derivative **10** as the intermediate. The *in situ* reduction of **10** with sodium bisulfite indeed provided the desired diselenide **6** in 54% yield (Scheme 7b). Similarly, the enolate of **9** was treated with freshly generated selenenyl chloride **10** to provide monoselenide **5** in 45% yield (Scheme 7c). The X-ray crystallography results further confirmed the structure of **5**.

Stability and photophysical properties of compounds **5** and **6**

With compounds **5** and **6** in hand, we first checked their stability. Their solutions in 1:9 DMSO/PBS (pH 7.4) were prepared and monitored. Under dark conditions, negligible amounts (<2%) of decomposition were noted after 3 days. Under normal indoor light conditions, only ~5% degradation after 24 h was observed, indicating that both compounds were stable enough for further studies. The photophysical properties of **5** and **6** were also measured (Fig. S5). The strong absorption peaks were observed for compounds **5** and **6** at $\lambda_{\text{max}} = 321 \text{ nm}$ and $\lambda_{\text{max}} = 324 \text{ nm}$, respectively. However, neither appeared to be fluorescent.



Scheme 8 Photolysis of compounds **5** and **6**.

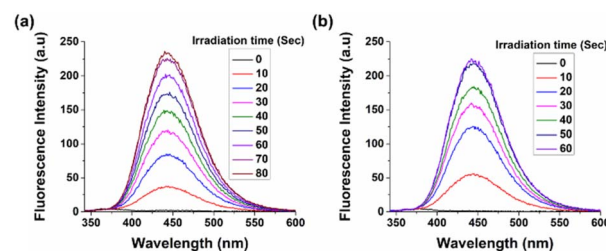


Fig. 1 Fluorescence spectra of (a) naphthacyl monoselenide **5** and (b) naphthacyl diselenide **6** ($E_x = 320 \text{ nm}$) under irradiation with LED light at regular intervals of time (10 s).

Photoreactions of compounds **5** and **6**

We next carried out their photoreactions (under 365 nm LED light). The reactions appeared to be much faster (completed within 4 min) than that of nitrobenzyl derivatives **1** and **2** (~300 min for completion) under the same conditions. The formation of the photoproduct **11** was completed in a few minutes with 76% or 72% yields (Scheme 8, Fig. S3 and S4) from compound **5** and **6**, respectively. We also observed the formation of elemental selenium in the reaction, indicating the formation of $\text{H}_2\text{Se}/\text{H}_2\text{Se}_2$ in the process.

Since photoproduct **11** is a fluorescent molecule,²⁹ we could use fluorescence spectroscopy to monitor the photo-uncaging progress. As shown in Fig. 1, the solutions of compounds **5** and **6** (100 μM in 10% DMSO-PBS at 50 mM, pH 7.4) were subjected to the 365 nm LED light at regular time intervals (10 s). A clear time-dependent increase of fluorescence intensity

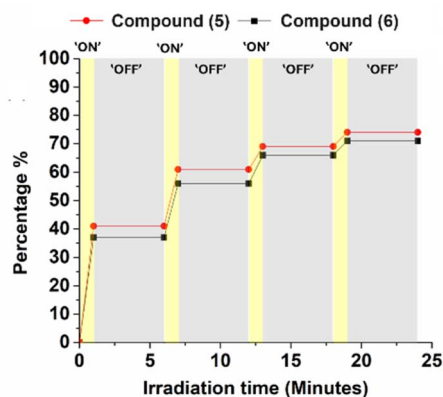
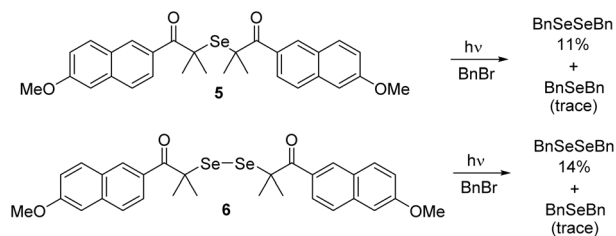
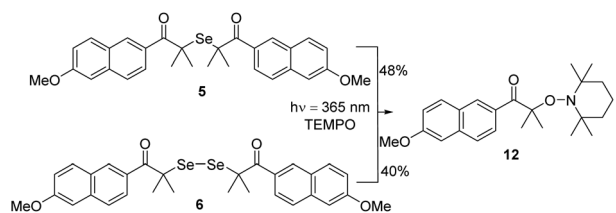


Fig. 2 Photoreaction of compounds **5/6** under 'light' and 'dark' conditions for regular intervals of time.





Scheme 9 Trapping experiment with BnBr.



Scheme 10 Radical trapping experiments with TEMPO.

was noted. The spectra also matched the authentic spectrum of compound **11**.

To further demonstrate the spatiotemporal control of the photo-uncaging process, we carried out 'light on-off' experiments with compounds **5** and **6**, in which the compounds were exposed to 'light' and 'dark' conditions over regular intervals of time. The formation of the photoproduct **11** was quantified by $^1\text{H-NMR}$ analysis. As shown in Fig. 2, under the 'dark' condition, the photo-uncaging process completely ceased and

only proceeded under the 'light on' condition. These results indicated that the reaction was solely controlled by the light.

H_2Se and H_2Se_2 trapping studies

To confirm the release of H_2Se and H_2Se_2 from compounds **5** and **6** under light, trapping experiments with benzyl bromide were performed. Briefly, the solutions of **5** and **6** were exposed to light irradiation for 20 min in the presence of BnBr. In both cases, BnSeSeBn was the main trapped product (isolated yield of 11% and 14%, respectively) with trace amounts of BnSeBn (Scheme 9). The formation of BnSeSeBn from compound **5** was probably due to the autooxidation of BnSeH. The formation of BnSeSeBn provided direct evidence for $\text{H}_2\text{Se}/\text{H}_2\text{Se}_2$ release from compounds **5** and **6**. We also carried out the control experiment (*i.e.* treating BnBr with elemental selenium Se^0 under the same condition). However, we did not observe the formation of BnSeSeBn under such conditions, further confirming the photo-triggered release of $\text{H}_2\text{Se}/\text{H}_2\text{Se}_2$.

Radical trapping experiment

We envisioned the photoreaction of compounds **5** and **6** was through a radical process, similar to that of naphthacyl-sulfur

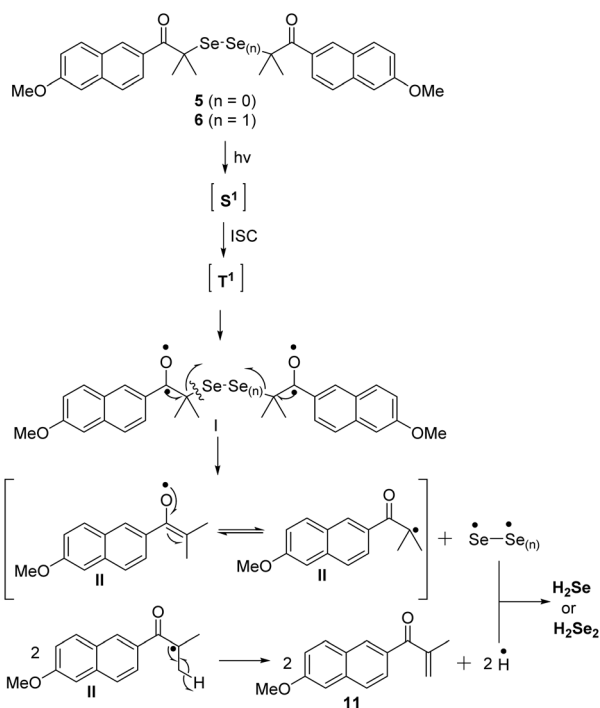
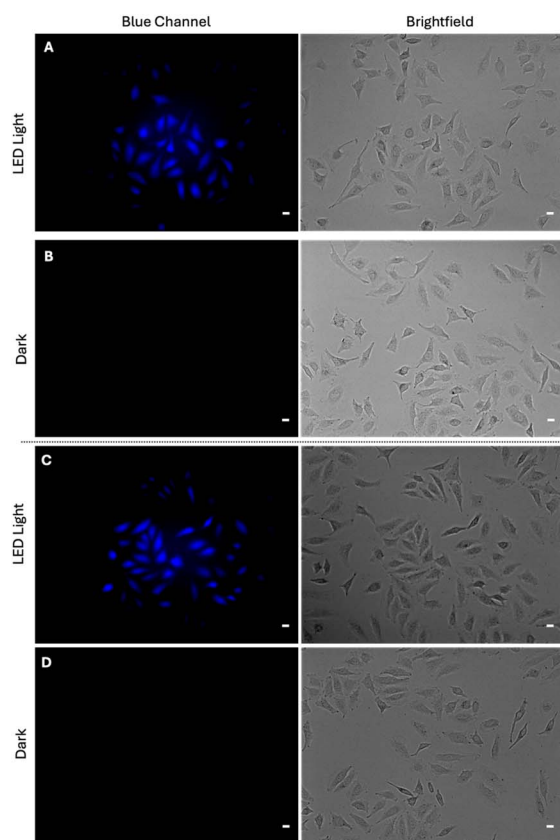
Scheme 11 Proposed mechanism of $\text{H}_2\text{Se}_2/\text{H}_2\text{Se}$ formation from **5** and **6**.

Fig. 3 Representative images of HeLa cells. Cells were treated with (A and B) compound **5** ($30\ \mu\text{M}$) or (C and D) compound **6** ($10\ \mu\text{M}$) for 30 min at $37\ ^\circ\text{C}$, 5% CO_2 . After incubation, cells were (B and D) washed three times with PBS and subjected to imaging or (A and C) washed once with PBS, subjected to LED light for 2 min, and then washed twice with PBS before fluorescence imaging occurred. Scale bars = $20\ \mu\text{m}$.



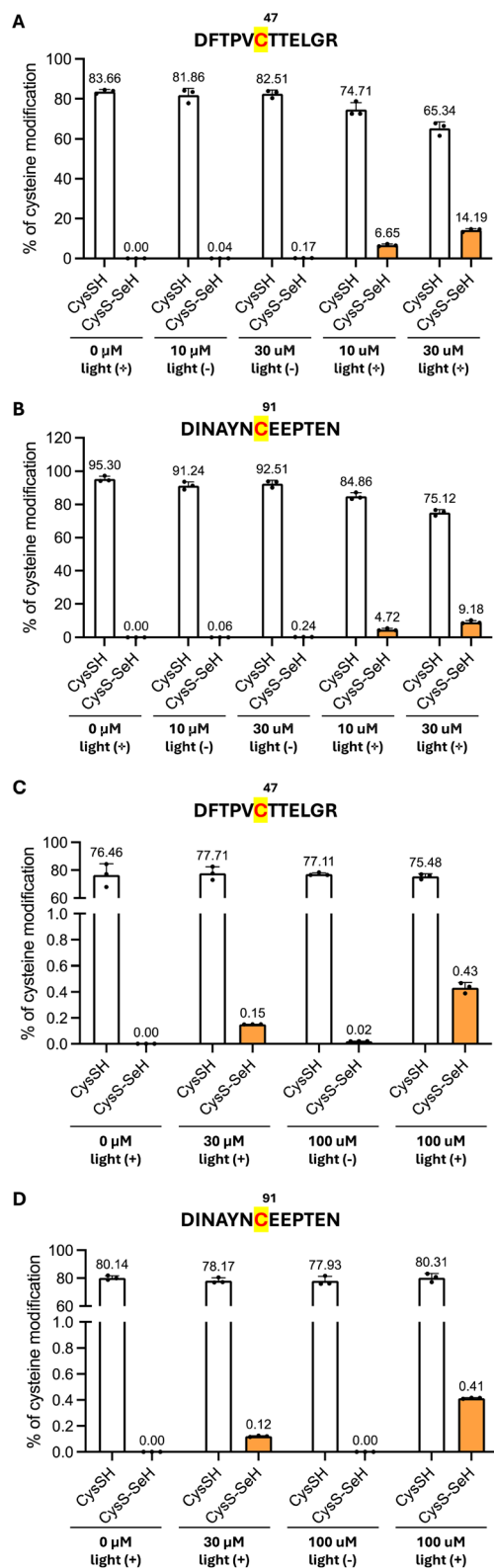


Fig. 4 Mass spectrometry analyses of the percentage of cysteine residue post-translational modifications at Cys47 and Cys91 in (A and B) recombinant PRDX6 treated with a final concentration of 0, 10, and 30 μ M of compound 5 \pm LED light irradiation for 2 min and (C and D) PRDX6-overexpressing HEK293T cells treated with 0, 30, or 100 μ M of compound 5, incubated for 30 min at 37 $^{\circ}$ C, washed with PBS, and then subjected to \pm LED light irradiation for 4 min. PBS was then

compounds.^{29–31} To demonstrate this, we carried out radical trapping experiments using TEMPO (Scheme 10). In both cases, the naph-TEMPO adduct **12** was obtained in moderate yields. This confirmed the formation of the carbon radical in the reaction, also indicating Se radical formation in the process.

Photouncaging mechanism

Upon irradiation, compound **5** or **6** first reach the singlet excited state (*via* $n \rightarrow \pi^*$ transition), then undergo intersystem crossing (ISC) to the triplet state. In this state, the carbonyl group generates a diradical intermediate **I** (Scheme 11). From this intermediate, the C–Se bond cleaves, forming intermediate-**II** and the Se radical. Intermediate-**II** subsequently releases a hydrogen radical, yielding the photoproduct **11**. The released H-radical combines with the selenium radical to produce H_2Se or H_2Se_2 .

Photo-triggered H_2Se/H_2Se_2 release in cells

We next wanted to determine whether compounds **5** and **6** could generate H_2Se/H_2Se_2 in cells after photoirradiation. Briefly, HeLa cells were treated with the compounds (10 or 30 μ M) for 30 min at 37 $^{\circ}$ C, 5% CO_2 and then washed with PBS before being subjected to LED light irradiation for 2 min. The cells were then washed with PBS again before being subjected to fluorescence microscopy. Strong blue fluorescence was observed in both treatments with light irradiation (Fig. 3A and C), thus confirming that the photo uncaging of **5** and **6** (and subsequent release of H_2Se/H_2Se_2) to form photoproduct **11** could be induced in cellular systems.

Protein S-selenylation on PRDX6 (recombinant protein and in HEK293T cells)

We next wondered whether our donors could be used to induce S-selenylation (forming CysS-SeH) on proteins. This post-translational modification, particularly on peroxiredoxin 6 (PRDX6), has recently received major attention in the field.^{14,15,33} Several studies have found that S-selenylation on PRDX6's Cys47 is responsible for PRDX6 being a selenium-acceptor protein that facilitates intracellular selenium utilization and effectively guides ferroptosis sensitivity. In those studies, recombinant PRDX6 was treated with Na_2SeO_3 +GSH, or with $Na_2Se + H_2O_2$ to induce S-selenylation. Those reactions, however, are complex and can also produce other oxidized selenium/selenide species and in turn affect the efficacy of S-selenylation. Thus, we wondered whether we could use our photo-controlled method of producing H_2Se to induce protein S-selenylation in a more controlled and effective manner.

In our studies, recombinant PRDX6 was treated with 0, 10, or 30 μ M of compound **5**, irradiated with LED light for 2 min (or

changed to the cell culture media, and cells were incubated for an additional 30 min at 37 $^{\circ}$ C before being lysed and alkylated with IAM followed by immunoprecipitation. Data is represented as mean \pm S.D. ($n = 3$).



kept in the dark), and then incubated for 30 min at room temperature in the dark. Samples were subsequently alkylated with iodoacetamide (IAM), digested with trypsin, and then subjected to liquid chromatography-electrospray ionization-quadrupole time-of-flight tandem mass spectrometry (LC-ESI-Q-TOF MS/MS) according to previously reported procedures.³³ Target peptides and modification levels of each cysteine residue were determined. As shown in Fig. 4A, we observed a concentration-dependent increase in CysS-SeH formation at the active-site cysteine (Cys47, sequence: DFTPVCITTELGR) of PRDX6. The percentage of cysteine modification was 6.65% and 14.19% for the 10 and 30 μM treatments of compound 5 under light irradiation, respectively. These results were similar to the $\sim 9\%$ reported by Fujita *et al.*³³ through their incubation of PRDX6 with Na_2SeO_3 and GSH, indicating our donor's comparable efficiency. Notably, our donor not only modified the active site cysteine, but also generated CysS-SeH at PRDX6's non-active site cysteine residue (Cys91, sequence: DINAYNCEPTEN) (Fig. 4B). We observed a 4.72% and 9.18% cysteine modification to CysS-SeH with the 10 and 30 μM compound 5 treatments, respectively.

As compound 5 could be used for fluorescence imaging in live cells and could induce S-selenylation in recombinant PRDX6, we next attempted to induce these protein modifications in PRDX6-overexpressing HEK293T cells. After 48 hours post-transfection of HEK293T cells with human PRDX6 plasmid (pcDNA3.2-FLAG-His-PRDX6), cells were treated with 0, 30, or 100 μM of compound 5 in serum- and cystine-free DMEM for 30 min at 37 $^\circ\text{C}$, washed with PBS, and then subjected to LED light irradiation for 4 min. Cells not irradiated with light served as the control. Next, the cell media was changed (DMEM, FBS and cystine-free), and the cells were incubated for 30 min at 37 $^\circ\text{C}$. They were then lysed with RIPA buffer containing 10 mM IAM, immunoprecipitation was performed, and samples were analyzed by mass spectrometry following the same method as above. Interestingly, we detected 0.15% and 0.43% of CysS-SeH modifications on Cys47 (Fig. 4C) after cells were treated 30 μM and 100 μM of compound 5, respectively, under LED light. Similarly, 0.12% and 0.41% of CysS-SeH was detected at Cys91 (Fig. 4D) after treatment with 30 μM and 100 μM of compound 5, respectively, under light irradiation conditions. As these percent modifications were not very high, we also quantified the amount of PRDX6 expressed in wild type (WT) and PRDX6-overexpressing HEK293T cells (8.3 ng for 1 μg of cell lysate) by western blotting (Fig. S6). To the best of our knowledge, this is the first time CysS-SeH modifications have been induced and detected on proteins (*i.e.* PRDX6) expressed in cells.

Conclusions

In this work, we explored light responsive $\text{H}_2\text{Se}/\text{H}_2\text{Se}_2$ donors by utilizing two different PRPGs: 2-nitrobenzyl selenides and 2-methoxy-6-naphthacyl selenides. 2-Nitrobenzyl selenides were found to release $\text{H}_2\text{Se}/\text{H}_2\text{Se}_2$ slowly under UV light. The released H_2Se was also found to react with the photoproduct *o*-nitroso benzaldehyde. Therefore, the 2-nitrobenzyl template

was determined to be unsuitable for the design of photo-triggered H_2Se donors. On the other hand, naphthacyl selenides were found to undergo clean and fast photoreactions to produce $\text{H}_2\text{Se}/\text{H}_2\text{Se}_2$ and a blue fluorescent photoproduct. The radical-based reaction mechanism was proved by TEMPO trapping studies. This self-monitoring and quick releasing ability make naphthacyl selenides 'smart donors' for biological applications. We also demonstrated the biological applicability of our compounds by applying them for fluorescence imaging in cells and achieved S-selenylation (CysS-SeH) on recombinant PRDX6, in accordance with previously reported studies.^{14,15,33} Significantly, we were also able to induce CysS-SeH on PRDX6 expressed in live HEK293T cells after treatment with compound 5 and subsequent light irradiation. To the best of our knowledge, this is the first report of selenium incorporation at cysteine residues under such cellular conditions. We believe that our light-responsive donors will serve as valuable tools and concepts for inducing post-translational modifications on proteins, provide new insights into their biological functions, and aid in efforts to elucidate the intricacies of cellular selenium metabolism and ferroptosis regulation. It should also be noted that H_2Se is a highly reactive and unstable species. Once it is produced (whether it be from donors or *via* endogenous formation pathways), it can be rapidly oxidized to other selenium species such as Se^0 . All these species may lead to biological consequences. Therefore, understanding the timing of H_2Se formation from the donors, as well as the possible reactions with biomolecules for each Se species would be helpful for better understanding the applications of donor compounds.

Author contributions

B. R., E. D., T. A., and M. X. conceived the ideas and designed the studies. B. R., E. D., and S. Z. carried out the synthesis. J. R. R. performed X-ray studies. M. S. carried out cell-based fluorescent imaging studies. M. S., S. O., M. J., H. F., and T. A. designed and performed protein S-selenylation studies. M. X., B. R., E. D., and M. S. wrote the manuscript. All authors reviewed and approved the final version of the manuscript.

Conflicts of interest

There are no conflicts to declare.

Data availability

The authors confirm that the data supporting the findings of this study are available within the article and its SI. Supplementary information: experimental protocols, compound characterizations, NMR spectra. See DOI: <https://doi.org/10.1039/d5sc05141j>.

CCDC 2380190, 2380191 and 2455512 contain the supplementary crystallographic data for this paper.³⁴



Acknowledgements

This work was supported by the NIH (R35GM149170) to M. X. M. S. is supported by a NIH F31 Predoctoral Fellowship (F31HL170516). It was also supported in part by Grants-in-Aid for Transformative Research Areas, International Leading Research, Scientific Research [(S), (A), (C), Challenging Exploratory Research] from the Ministry of Education, Culture, Sports, Sciences and Technology (MEXT), Japan, to T. Akaike (21H05263, 23K20040, 24H00063 and 22K19397), S. Ogata (23K14333) and M. Jung (23K14341); Japan Science and Technology Agency (JST), CREST Grant Number JPMJCR2024, Japan to T. Akaike; JST FOREST Program Grant Number JPMJFR230K, Japan to H. Fujita; and a grant from the Japan Agency for Medical Research and Development (AMED), Grant Number JP21zf0127001, Japan, to T. Akaike. X-ray diffraction experiments were performed with a diffractometer purchased through a grant through the NSF-MRI program (CHE-2117549) located at Brown University.

References

- (a) R. C. McKenzie, T. S. Rafferty and G. J. Beckett, *Immunol. Today*, 1998, **19**, 342–345; (b) D. L. Hatfield, P. A. Tsuji, B. A. Carlson and V. N. Gladyshev, *Trends Biochem. Sci.*, 2014, **39**, 112–120.
- J. S. Chen, *Asia Pac. J. Clin. Nutr.*, 2012, **21**, 320–326.
- D. Muller and H. Desel, *Hum. Exp. Toxicol.*, 2010, **29**, 431–434.
- H. J. Reich and R. J. Hondal, *ACS Chem. Biol.*, 2016, **11**, 821–841.
- R. L. Schmidt and M. Simonović, *Croat. Med. J.*, 2012, **53**, 535–550.
- N. Paton, A. Cantor, A. Pescatore, M. Ford and C. Smith, *Poult. Sci. J.*, 2002, **81**, 1548–1554.
- W. Hu, C. Zhao, H. Hu and S. Yin, *Nutrients*, 2021, **13**, 1739.
- H. E. Ganther, *Metabolism of Hydrogen Selenide and Methylated Selenides*. Springer eBooks 1979, pp. 107–128.
- K. Cupp-Sutton and M. Ashby, *Antioxidants*, 2016, **5**, 42.
- K. Samra, M. Kuganesan, W. Smith, A. Kleyman, R. Tidswell, N. Arulkumaran, M. Singer and A. Dyson, *Int. J. Mol. Sci.*, 2021, **22**, 3258.
- M. Kuganesan, K. Samra, E. Evans, M. Singer and A. Dyson, *Intensive Care Med. Exp.*, 2019, **7**, 71.
- M. S. Vandiver and S. H. Snyder, *J. Mol. Med.*, 2012, **90**, 255–263.
- (a) M. R. Filipovic, J. Zivanovic, B. Alvarez and R. Banerjee, *Chem. Rev.*, 2018, **118**, 1253–1337; (b) C. T. Yang, N. O. Devarie-Baez, A. Hamsath, X. D. Fu and M. Xian, *Antioxid. Redox Signaling*, 2020, **33**, 1092–1114.
- J. Ito, T. Nakamura, T. Toyama, D. Chen, C. Berndt, G. Poschmann, A. S. D. Mourão, S. Doll, M. Suzuki, W. Zhang, J. Zheng, D. Trümbach, N. Yamada, K. Ono, M. Yazaki, Y. Kawai, M. Arisawa, Y. Ohsaki, H. Shirakawa, A. Wahida, B. Proneth, Y. Saito, K. Nakagawa, E. Mishima and M. Conrad, *Mol. Cell*, 2024, **84**, 4629–4644.
- Z. Chen, A. Inague, K. Kaushal, G. Fazeli, D. Schilling, T. N. Xavier da Silva, A. F. dos Santos, T. Cheytan, F. P. Freitas, U. Yildiz, L. G. Viviani, R. S. Lima, M. P. Pinz, I. Medeiros, T. S. Iijima, T. G. P. Alegria, R. Pereira da Silva, L. R. Diniz, S. Weinzeig, J. Klein-Seetharaman, A. Trumpp, A. Mañas, R. Hondal, C. Bartenhagen, M. Fischer, B. K. Shimada, L. A. Seale, T. S. Chillon, M. Fabiano, L. Schomburg, U. Schweizer, L. E. Netto, F. C. Meotti, T. P. Dick, H. Alborzinia, S. Miyamoto and J. P. Friedmann Angeli, *Mol. Cell*, 2024, **84**, 4645–4659.
- (a) C. R. Powell, K. M. Dillon and J. B. Matson, *Biochem. Pharmacol.*, 2018, **149**, 110–123; (b) Y. Zheng, B. Yu, L. K. De La Cruz, M. Roy Choudhury, A. Anifowose and B. Wang, *Med. Res. Rev.*, 2018, **38**, 57–100; (c) Y. Zhao, T. D. Biggs and M. Xian, *Chem. Commun.*, 2014, **50**, 11788–11805.
- L. Li, M. Whiteman, Y. Y. Guan, K. L. Neo, Y. Cheng, S. W. Lee, Y. Zhao, R. Baskar, C.-H. Tan and P. K. Moore, *Circulation*, 2008, **117**, 2351–2360.
- W. Feng, X.-Y. Teo, W. Novera, P. M. Ramanujulu, D. Liang, D. Huang, P. K. Moore, L.-W. Deng and B. W. Dymock, *J. Med. Chem.*, 2015, **58**, 6456–6480.
- T. D. Newton and M. D. Pluth, *Chem. Sci.*, 2019, **10**, 10723–10727.
- T. D. Newton, S. G. Bolton, A. C. Garcia, J. E. Chouinard, S. L. Golledge, L. N. Zakharov and M. D. Pluth, *J. Am. Chem. Soc.*, 2021, **143**, 19542–19550.
- T. D. Newton, K. Li, J. Sharma, P. A. Champagne and M. D. Pluth, *Chem. Sci.*, 2023, **14**, 7581–7588.
- R. A. Hankins, M. E. Carter, C. Zhu, C. Chen and J. C. Lukesh, *Chem. Sci.*, 2022, **13**, 13094–13099.
- (a) X. Kang, H. Huang, C. Jiang, L. Cheng, Y. Sang, X. Cai, Y. Dong, L. Sun, X. Wen, Z. Xi and L. Yi, *J. Am. Chem. Soc.*, 2022, **144**, 3957–3967; (b) W. Liang, Y. Dong and L. Yi, *Anal. Chem.*, 2025, **97**, 16104–16109.
- Y. Dong, W. Liang and L. Yi, *J. Am. Chem. Soc.*, 2024, **146**, 24776–24781.
- (a) J. Y. C. Chu, D. G. Marsh and W. H. H. Guenther, *J. Am. Chem. Soc.*, 1975, **97**, 4905–4908; (b) W. Stanley, M. R. VanDeMark and P. L. Kumler, *J. Chem. Soc., Chem. Commun.*, 1974, 700–701.
- A. P. Welegedara, L. A. Adams, T. Huber, B. Graham and G. Otting, *Bioconjugate Chem.*, 2018, **29**, 2257–2264.
- P. Klán, T. Šolomek, C. G. Bochet, A. Blanc, R. Givens, M. Rubina, V. Popik, A. Kostikov and J. Wirz, *Chem. Rev.*, 2012, **113**, 119–191.
- W. W. Paudler and A. G. Zeiler, *Chem. Commun.*, 1967, 1077–1078.
- B. Roy, M. Shieh, S. Xu, X. Ni and M. Xian, *J. Am. Chem. Soc.*, 2022, **145**, 277–287.
- B. Roy, M. Shieh, T. Takata, M. Jung, E. Das, S. Xu, T. Akaike and M. Xian, *J. Am. Chem. Soc.*, 2024, **146**, 30502–30509.



- 31 B. Roy, R. Kojima, O. Shah, M. Shieh, E. Das, S. Ezzatpour, E. Sato, Y. Hirata, S. Lindahl, A. Matsuzawa, H. C. Aguilar and M. Xian, *Redox Biol.*, 2025, **79**, 103475.
- 32 H. J. Reich, C. A. Hoeger and W. W. Willis, *Tetrahedron*, 1985, **41**, 4771–4779.
- 33 H. Fujita, Y. Tanaka, S. Ogata, N. Suzuki, S. Kuno, U. Barayeu, T. Akaike, Y. Ogra and K. Iwai, *Nat. Struct. Mol. Biol.*, 2024, **31**, 1277–1285.
- 34 B. Roy, E. Das, M. Shieh, S. Ogata, M. Jung, H. Fujita, S. Zhang, J. R. Robinson, T. Akaike and M. Xian, CCDC 2380190: Experimental Crystal Structure Determination, 2025, DOI: [10.5517/ccdc.csd.cc2kwsbl](https://doi.org/10.5517/ccdc.csd.cc2kwsbl); B. Roy, E. Das, M. Shieh, S. Ogata, M. Jung, H. Fujita, S. Zhang, J. R. Robinson, T. Akaike and M. Xian, CCDC 2380191: Experimental Crystal Structure Determination, 2025, DOI: [10.5517/ccdc.csd.cc2kwsem](https://doi.org/10.5517/ccdc.csd.cc2kwsem); B. Roy, E. Das, M. Shieh, S. Ogata, M. Jung, H. Fujita, S. Zhang, J. R. Robinson, T. Akaike and M. Xian, CCDC 2455512: Experimental Crystal Structure Determination, 2025, DOI: [10.5517/ccdc.csd.cc2nf52c](https://doi.org/10.5517/ccdc.csd.cc2nf52c).

